Optical properties of gold clusters in the size range 2–4 nm

B. Palpant
Laboratoire de Spectrométrie Ionique et Moléculaire, Université Claude Bernard Lyon 1, 43 boulevard du 11 novembre 1918, 69622 Villeurbanne Cedex, France

B. Prével
Département de Physique des Matériaux, Université Claude Bernard Lyon 1, 43 boulevard du 11 novembre 1918, 69622 Villeurbanne Cedex, France

J. Lermé, E. Cottancin, and M. Pellarin
Laboratoire de Spectrométrie Ionique et Moléculaire, Université Claude Bernard Lyon 1, 43 boulevard du 11 novembre 1918, 69622 Villeurbanne Cedex, France

M. Treilleux and A. Perez
Département de Physique des Matériaux, Université Claude Bernard Lyon 1, 43 boulevard du 11 novembre 1918, 69622 Villeurbanne Cedex, France

J. L. Vialle and M. Broyer
Laboratoire de Spectrométrie Ionique et Moléculaire, Université Claude Bernard Lyon 1, 43 boulevard du 11 novembre 1918, 69622 Villeurbanne Cedex, France

(Received 19 June 1997)

We report experiments on gold clusters in the size range 2–4 nm, embedded in an alumina matrix. The metallic particles are produced with a laser vaporization source and codeposited with a dielectric vapor as a thin film on a substrate. Our technique allows varying the cluster size at a given metal concentration. These composite materials are studied through optical absorption and ellipsometric measurements, allowing determination of their complex index of refraction. Various complementary techniques provide information about their morphology, their chemical composition, the thickness of the films, and the size distribution of the clusters. The surface plasmon resonance in the absorption spectra is shown to be damped and blueshifted with decreasing cluster size. Theoretical calculations in the framework of the time-dependent local-density approximation allow a clear understanding of these experimental results. [S0163-1829(98)00703-6]

I. INTRODUCTION

The optical response of clusters directly reflects their electronic structure, which strongly depends on the particle size and shape. One can study this response by direct investigations on free clusters,[1–5] or by deposition of nanoparticles on substrates.[6] In an alternative approach, embedding clusters in a dielectric matrix not only opens new material outlooks with particular properties, but is also a simple way to study the optical response of the nanoparticles.[7] Actually these specific optical properties are well known and used for many centuries in art glassware.[8]

Such nanostructured materials are produced and studied by many different techniques, as colloidal solution investigations,[9–12] sol-gel or chemical synthesis,[13–17] cosputtering,[18–21] electrochemical deposition,[22,23] ion implantation,[24–27] electron-beam lithography,[28] or low-energy cluster-beam deposition (LECBD).[29–31] One of the main advantages of this last technique is that it allows one to independently control the cluster size and the metal concentration in the films.

The main feature in the optical response is the surface plasmon excitation (collective oscillation of the conduction electrons), resulting in a resonance band in the absorption spectra. For gold as well as for the other noble metals, the plasmon resonance occurs in the near-UV/visible region. It is therefore easier to perform the experimental optical study of such metal nanoparticles, and also interesting to use them for optical-device applications.

In our laboratory, clusters of a wide range of elements can be produced by means of a laser vaporization source. They can be deposited on a substrate by the LECBD technique and embedded in an insulator matrix, leading to the formation of thin films of nanocomposite materials. Samples consisting of spherical gold nanoparticles in an amorphous Al_2O_3 matrix were prepared, with different cluster size distributions and a metal volumic fraction of about 4%.

Several characterization techniques, namely, Rutherford back-scattering (RBS), alpha-step measurements, x-ray diffraction, and transmission electron microscopy (TEM), provide valuable information about the film morphology, the matrix stoichiometry and its porosity, the crystallinity of both compounds, the metal concentration, and the film thickness.

The central task of this paper is focused on the optical absorption and ellipsometric measurements, which both reveal a size-dependent behavior. The main features consist of a blueshift and a damping of the plasmon resonance band with decreasing cluster radius. The complex index of refraction of each thin film sample was extracted from the ellipso-

metric data, by means of minimization calculations. These results are compared with the Maxwell-Garnett effective medium model.[32]

Theoretical time-dependent local-density-approximation (TDLDA) calculations have been carried out to interpreting the experimental results. In the model, the electronic density spill-out effect, the embedding matrix index, and the influence of *d* electrons were included in order to describe the cluster optical properties in the most realistic way.

The paper content is organized as follows. The sample production and characterization are reported in Sec. II, and the absorption and ellipsometric experimental results in Secs. IV and V, respectively. Section III outlines classical approaches of the optical properties of the composite films. An interpretation of the size-dependent behavior, provided by the TDLDA investigations, is discussed in Sec. VI.

II. SAMPLE PRODUCTION AND CHARACTERIZATION

The experimental setup has been previously described in detail.[31] The cluster source is a laser vaporization one, where the beam of a frequency-doubled Nd:Yag pulsed laser is focused onto a rod of the element to be studied. The atomic plasma is thermalized by helium gas and expands into vacuum through a nozzle. For the present study we used either high-pressure helium delivered by a pulsed valve, or a continuous helium flow at lower pressure (few tens of mbar). The pressure conditions allow us to control the free cluster size and thus to obtain samples with different size distributions.

The neutral clusters then pass through a skimmer into a high-vacuum chamber where they may be photoionized and analyzed by means of a reflectron time-of-flight mass spectrometer. The size-resolved mass distribution reveals the same magic number series as that predicted by the jellium model,[33,34] which means that the gold clusters produced by the source at room temperature are probably spherical.

The clusters are finally deposited on a substrate in a vacuum chamber (10^{-7} mbar), simultaneously with the dielectric matrix evaporated with an electron gun. We can check the volumic fraction of metal by use of quartz balances, which provide both deposition rates. The film thickness depends on the kind of study to be performed, from 15 nm for TEM observations up to 200 nm for optical absorption analysis. Moreover, specific types of substrates are selected: amorphous carbon-coated grids for TEM, silicon wafers for ellipsometry and RBS, pure silica for optical absorption.

Preliminary experiments were first performed on pure alumina films (without any metallic cluster) in order to determine precisely the properties of the dielectric matrix and to optimize the experimental deposition conditions. Alpha-step thickness measurements and ellipsometric fits show an important porosity (about 40% with respect to crystalline Al_2O_3); the matrix morphology seems actually to be close to an anodic aluminum oxide one. RBS measurements reveal a slight overstoichiometry according to the formula $Al_2O_{3.2}$. Associated with alpha-step analysis, they confirm a low alumina density in good agreement with its porosity. Complementary x-ray diffraction experiments demonstrate the amorphous structure of the matrix.

Gold clusters in alumina composite materials were then synthesized in the optimized deposition conditions. In order to avoid correlation effects between the metallic particles in the optical response of the material, their volumic fraction was maintained between 1.5% and 6.5%. These values are confirmed by RBS and energy-dispersive x-ray analysis (EDX). TEM micrographs of our samples were also performed (Fig. 1). They show nearly spherical clusters randomly distributed in the matrix. The size distributions give mean values from 2.0 to 3.7 nm in diameter (or a mean number of atoms per cluster from about 300 to 3000) depending on the samples. x-ray diffraction analysis reveals the fcc crystalline structure of the particles.

Grazing-incidence small-angle x-ray scattering (GISAXS) measurements,[35] performed at the LURE facility (Orsay, France) confirm the cluster mean size and point out their sphericity as well as the absence of any spatial correlations.

III. OPTICAL RESPONSE: CLASSICAL APPROACH

Noble-metal nanoparticles exhibit an optical absorption band in the near UV/visible region. This band, the so-called surface plasmon resonance, is classically described as the oscillation of the conduction electron cloud with respect to the ionic background. The relevant quantity in a classical approach is the frequency-dependent dielectric function $\tilde{\varepsilon}$ of the metal. Theoretically, the Drude-Sommerfeld model and classical electrodynamics account for both the bulk dielectric function and the surface plasmon frequency.[36] For noble metals, $\tilde{\varepsilon}$ can be written in a first approximation as

$$\tilde{\varepsilon}(\omega)=1+\chi^s(\omega)+\chi^d(\omega), \tag{1}$$

where χ^s represents the Drude part of the dielectric susceptibility (*s* electrons) and χ^d the interband part (*d* electrons). This last term plays an important role in the plasmon resonance oscillation, as will be shown in Sec. VI. The Mie theory accounts for the interaction between an electromagnetic wave and a single metallic sphere in a uniform transparent medium.[37] The absorption, in the dipolar approximation, exhibits the surface plasmon resonance behavior, the eigenfrequency ω_s of which can be directly related to the Drude bulk plasmon eigenfrequency ω_p by

$$\omega_s=\frac{\omega_p}{\sqrt{2\varepsilon_m+\tilde{\varepsilon}^d(\omega_s)}}, \tag{2}$$

where $\tilde{\varepsilon}^d=1+\chi^d$ is the interband part of the dielectric function of the metal and ε_m the dielectric function of the surrounding insulator. One can notice that the effect of this matrix is to shift the plasmon resonance peak to lower energies than in the free-cluster case.

In order to describe composite materials, several effective medium theories have been developed by introducing the concept of an effective dielectric function ε_{eff} for the whole inhomogeneous medium.[7,32,38–41] In the Maxwell-Garnett (MG) theory,[32] ε_{eff} satisfies the equation

$$\frac{\varepsilon_{\text{eff}}-\varepsilon_m}{\varepsilon_{\text{eff}}+2\varepsilon_m}=q\frac{\tilde{\varepsilon}-\varepsilon_m}{\tilde{\varepsilon}+2\varepsilon_m}, \tag{3}$$

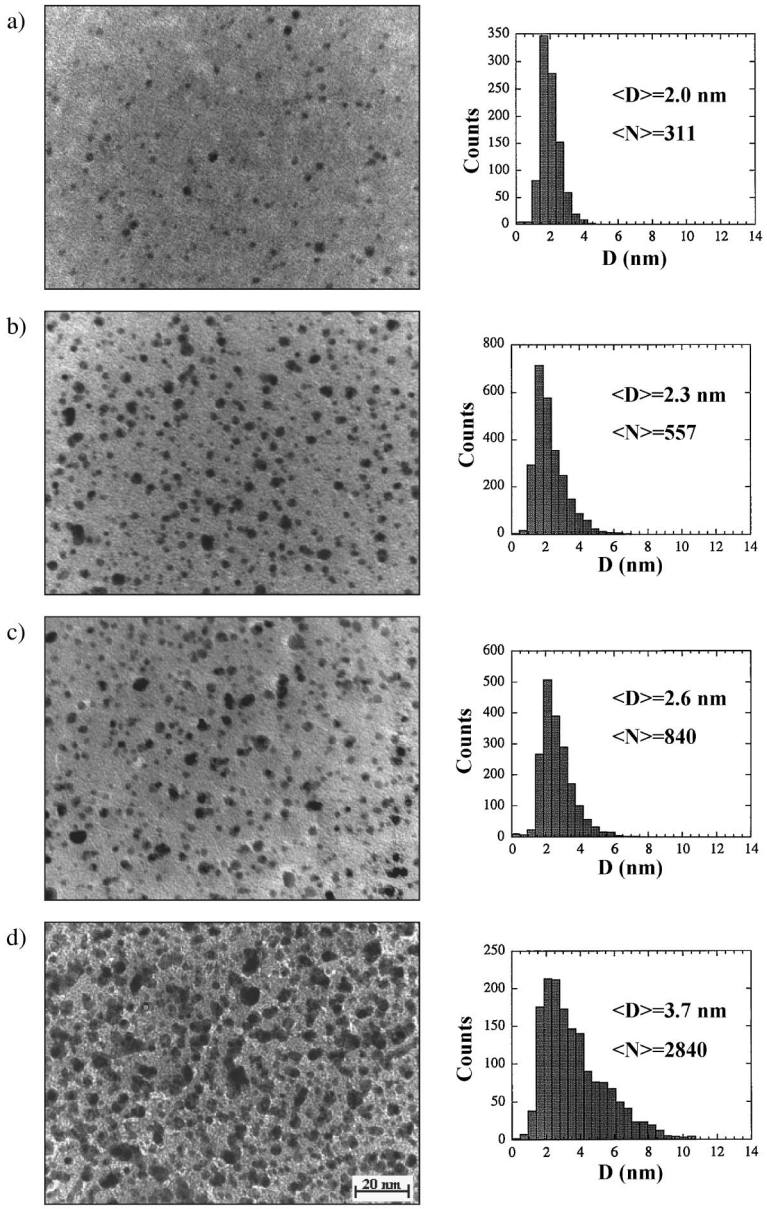

FIG. 1. TEM micrographs (at same scale) and the corresponding size distributions for four different samples (a)–(d). $\langle D \rangle$ is the mean diameter and $\langle N \rangle$ the mean number of atoms per cluster, deduced from the corresponding N distribution. The film thickness is about 15 nm. The metal concentration for each sample is 1.5% (a), 3.8% (b), 4.8% (c), and 6.5% (d). The different cluster sizes were obtained by modifying the source conditions and configuration.

where q is the volume fraction of the metallic particles. This theory has been used to analyze the optical response of our samples. It allows the calculation of the plasmon resonance peak shift when varying the q value, as long as these particles are spherical and sufficiently far from each other to limit local cluster-cluster interactions. This requires that q is less than about 10%. For our films q is in the range 1.5%–6.5%, corresponding to a resonance peak shift smaller than 0.01 eV. This means that no noticeable concentration effect is expected to underlie the differences between the optical responses of the different samples.

We have compared our experimental results with MG calculations involving the bulk dielectric function of gold given in Ref. 42 and the alumina dielectric function deduced from ellipsometry (see Sec. V). The evolution of the experimental optical spectra with respect to the measured mean cluster size, confronted to this bulk limit, will point out the size effects in the nanoparticle response.

IV. OPTICAL ABSORPTION

Absorption measurements were performed with a Varian double-beam spectrophotometer on the films deposited on pure silica (Suprasil) substrates, in the spectral range 200–1000 nm (1.24–6.2 eV). Results are shown in Fig. 2. The spectra present an absorption band lying around 2.4 eV due to the surface plasmon resonance. The absorption increases in the UV region, due to interband contributions.

These curves reveal a blueshift of the plasmon resonance peak with decreasing cluster size, from 2.33 eV for 3000 atoms per cluster to 2.52 eV for 300 atoms. Moreover, the lower value is blueshifted with respect to the MG value of 2.27 eV. One can also notice an increasing damping and broadening of the absorption band with decreasing cluster size, in agreement with recent results obtained by Whetten and co-workers on smaller clusters.[17] This behavior can be phenomenologically explained by the limitation of the mean free path of the conduction electrons when the cluster radius becomes smaller.[29,43] This size effect is also explained within

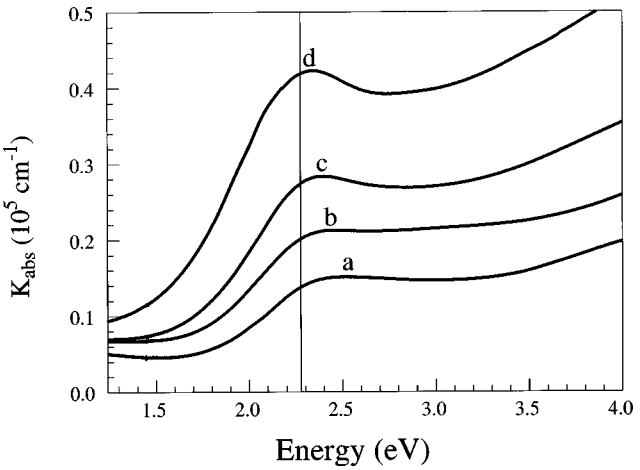

FIG. 2. Absorption coefficient K_{abs} vs energy, for four different samples whose labels correspond to those of the micrographs (Fig. 1). The vertical line indicates the bulk limit value given by the Maxwell-Garnett model.

the framework of quantum theories.[29,44,45] In addition, Kreibig and co-workers have pointed out the chemical-interface-damping effect in such matrix-embedded cluster materials.[29,43]

Figure 3 gives a comparison between the absorption spectrum of one of the samples [Fig. 2(d)] and the corresponding MG calculation. The finite-size effect on the optical response appears very clearly here: a blueshift and a damping of the measured resonance band with respect to those calculated with the bulk dielectric function. Note that part of the bandwidth in the experimental curves is also due to the cluster size dispersion in the nanostructured thin films.

An interpretation of the observed blueshift and damping of the resonance band will be given in Sec. VI.

V. ELLIPSOMETRIC MEASUREMENTS

In order to study the optical properties of our films we need to know their dielectric function or their complex refractive index. This dielectric function can be written as

$$\tilde{\varepsilon} = (n + ik)^2. \tag{4}$$

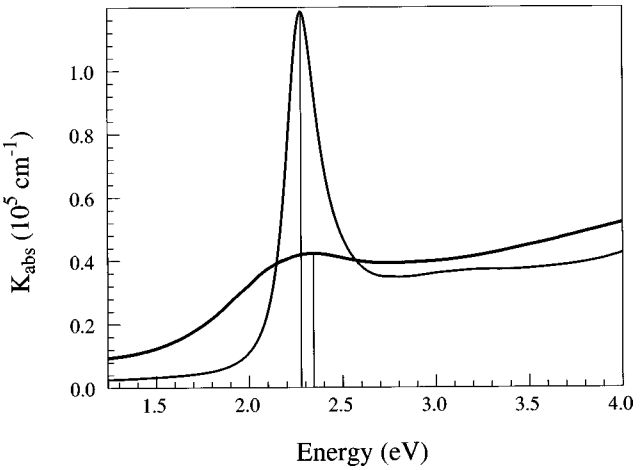

FIG. 3. Experimental (sample *d*, thick line) and simulated (Maxwell-Garnett model, thin line) absorption spectra.

The quantities n and k are linked together by the Kramers-Kronig relations; therefore, the knowledge of one of them allows *a priori* the determination of the other. This approach has already been used from either absorption or reflectivity experimental spectra,[46] but its accuracy is dependent on the spectral range of the measurements.

Another way consists in recording two experimental quantities depending on the complex refractive index. The minimization of the difference between the measured quantities and those calculated via a multilayer optical model (air, thin film, substrate) allows the determination of n and k.[47]

This led us to perform ellipsometric measurements. An incident polarized monochromatic light beam (wavelength from 240 to 700 nm) is reflected on the sample; its polarization changes and the collected beam intensity is measured with a photomultiplier through an analyzer, yielding the ellipsometric angles Ψ and Δ.[48–50] These experimental quantities are then compared with the calculated ones, expressed as a function of the indices n and k of the thin film. The least-square value (χ^2) is minimized by means of the simplex method.[51]

Pure alumina films were first investigated in order to determine the experimental dielectric function ε_m taken into account in the MG calculations (Secs. III and IV). Ψ and Δ were then measured for the cluster material samples. The optical model in which the film dielectric function is calculated with bulk gold data fits the experimental curves very well in the near-UV region. This indicates that to a first approximation, the dielectric function of the gold clusters nearly equals that of the bulk from 3.0 to 6.0 eV. It allowed us to reevaluate the values of the thickness e and the metallic concentration q of the thin films by χ^2 minimization in this spectral range. The values found are very close to those previously determined during deposition (rectified according to the porosity).

Finally, we calculated n and k for each wavelength by χ^2 minimization. Results are shown in Fig. 4. They reveal the same features as those observed in the optical absorption experiments: a size-dependent blueshift, a damping, and a broadening of the plasmon resonance band.

VI. THEORETICAL INTERPRETATION

TDLDA model calculations have been worked out in order to interpret the experimental findings.[52] In the model the conduction *s* electrons, responsible for the surface plasmon excitation, are quantum mechanically treated, whereas the ionic background is phenomenologically described as both (i) a positive charge distribution (jellium approximation) and (ii) a continuous polarizable medium that screens the electron-electron and electron-jellium Coulomb interactions inside the cluster. The screening due to the surrounding transparent matrix is taken into account by using the experimental dielectric function $\varepsilon_m(\omega)$ of bulk alumina[42] ($\varepsilon_m \approx 3.1$ in the relevant energy range).

The frequency-dependent dielectric function $\tilde{\varepsilon}^d(\omega)$ of the polarizable inner medium (mainly underlied by the fully occupied *d* band) was extracted from the experimental complex refractive index of bulk gold[42] through a Kramers-Kronig

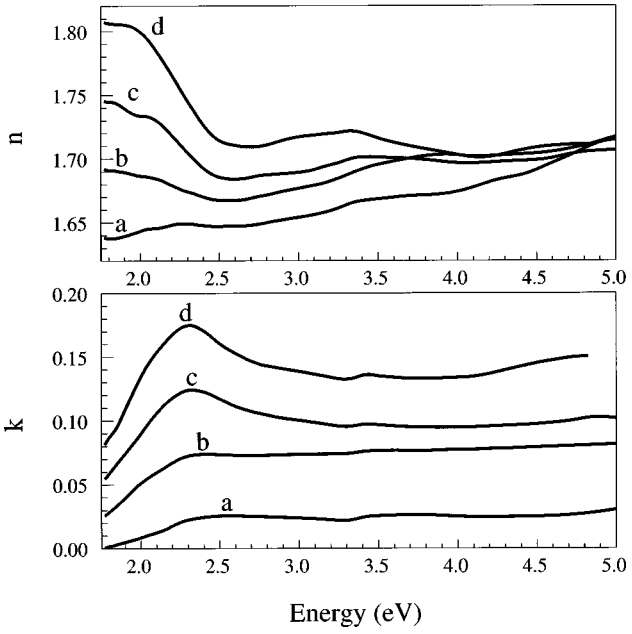

FIG. 4. Index of refraction n (upper figure) and index of extinction k (lower figure) versus energy for the different samples, calculated from ellipsometry analysis.

analysis, according to the procedure used for silver in Ref. 53. In contrast to alkali species, where only the valence s electrons have to be considered, the mutual polarization of the s- and d-electron clouds is essential for correctly predicting the magnitude of the surface plasmon frequency from Eq. (2), namely, $\omega_s \approx 2.5$ eV for $\varepsilon_m = 1$ [$\mathrm{Re}\tilde{\varepsilon}^d(\omega) \approx 10$ in the relevant energy range]. The simple jellium model [where $\mathrm{Re}\tilde{\varepsilon}^d(\omega) = 1$] yields the value $\omega_s \approx 5.2$ eV for large free gold clusters. Moreover, since the interband threshold for gold lies about 2 eV (below ω_s), Eq. (2) indicates that, contrary to silver where $\mathrm{Im}\tilde{\varepsilon}^d(\omega) = 0$ in the plasmon energy range, the resonance will be considerably broadened by the coupling with the interband transition [$\mathrm{Im}\tilde{\varepsilon}^d(\omega) > 0$ for $\omega > 2$ eV in the case of gold]. Let us emphasize, however, that only the influence of the polarizability and absorption properties of the core electrons on the s-electron excitations is taken into account in the present model. The real interband transitions, as obtained by applying classical Mie or MG absorption formula with the dielectric function of bulk gold (see Fig. 3), are thus not reproduced by the present TDLDA calculations.

Exhaustive calculations on free and embedded closed-shell Au_N clusters (size range $N = 8-440$) have been performed to analyze the respective influence of each model ingredient on the plasmon resonance. We briefly outline the main qualitative results of this study.

As for silver clusters the blueshift of ω_s with decreasing cluster size is explained by assuming that the screening effects due to the polarizable inner medium vanishes in the ''rind'' region of the particle, namely, by prescribing the condition $\tilde{\varepsilon}^d(R-a<r<R) = 1$ in the ionic background parametrization (R is the cluster radius). The vanishing tail of the localized d wave functions at the edge of the Wigner-Seitz cell brings some support to this assumption.[54] This ingredient was earlier introduced in a classical Mie analysis of the absorption spectra of Ag_N clusters embedded in rare-gas matrices,[18] and for interpreting the positive slope in the wave-vector surface plasmon dispersion of flat Ag surfaces.[55] In recent works devoted to silver clusters this two-region dielectric model was successfully (at least qualitatively) applied in various theoretical approaches, namely, in analytical Thomas-Fermi[54] and TDLDA (Ref. 56) model calculations. Indeed if the polarizable medium extends over the whole cluster volume ($0<r<R$) a redshift with decreasing cluster size is obtained instead. This redshift, due to the electron spill-out effect, essential for interpreting the optical absorption of simple metal clusters, is, however, very tiny due to strong screening (large $|\tilde{\varepsilon}^d|$ value). The introduction of the rind region increases the plasmon frequency and, above all, ensures a blueshift with decreasing cluster size. This size-dependent effect can be understood, in a very crude picture, by comparing the volumic ratio between the inner region of the cluster [$|\tilde{\varepsilon}^d| \gg 1$; low ω_s value from Eq. (2)] and the ''rind'' region ($\varepsilon^d = 1$; larger ω_s value).

Strictly speaking the thickness a has to be considered as a free phenomenological parameter. In view of the crude approximation consisting in replacing the discrete ionic structure by continuous step-walled jellium and polarizable media, a rigorous prescription for setting its value cannot be defined. For silver the thickness value, roughly estimated by Kresin by comparing the Wigner-Seitz radius r_s with the spatial extent of the radial d wave function, is 2 a.u.[54] Obviously the estimation depends on the threshold for which the d-electron density is assumed to be negligible. In TDLDA calculations carried out on the cluster Ag_{59}^+, assuming $a = 2$ a.u. seems to reproduce fairly nicely the experimental photoabsorption spectrum.[56] This value is also of the same order of magnitude as the one used by Liebsch to fit experimental results on Ag for both flat surfaces and clusters.[55]

Calculations involving nonlocal norm-conserving pseudopotentials show that the tails of the d wave functions are quite similar for Ag and Au atoms.[57] Since the r_s values of these two species are very close ($r_s = 3.02$ and 3.01 a.u. for Ag and Au, respectively), $a = 2$ a.u. is a reasonable value to perform our TDLDA investigations on gold clusters. Due to the above-mentioned approximations, introducing a size-dependent thickness would be an arbitrary refinement.

Indeed the blueshift is obtained also by a classical optical model involving the Mie-like formula relevant to a coated sphere, as done in Ref. 18. For free and embedded clusters the blueshifts calculated with this classical method are, however, slightly different from the TDLDA results, and obviously do not exhibit large size-to-size fluctuations superimposed on the mean trend. Moreover, a classical model disregards the quantum-mechanical effects occurring at both interfaces, such as, for instance, the electron spill-out at the outer one, which may balance partly the blueshift.

Figures 5 and 6 illustrate the above discussion. We comment only on additional features. In Fig. 5 one can see that, as compared to the optical response in vacuum, the plasmon peak redshift induced by the surrounding alumina matrix is rather small because $|\tilde{\varepsilon}^d|$ is large compared to ε_m [see Eq. (2)]. The width of the surface plasmon resonance is found strongly correlated with its location relative to the interband threshold. The large width observed, resulting from the large

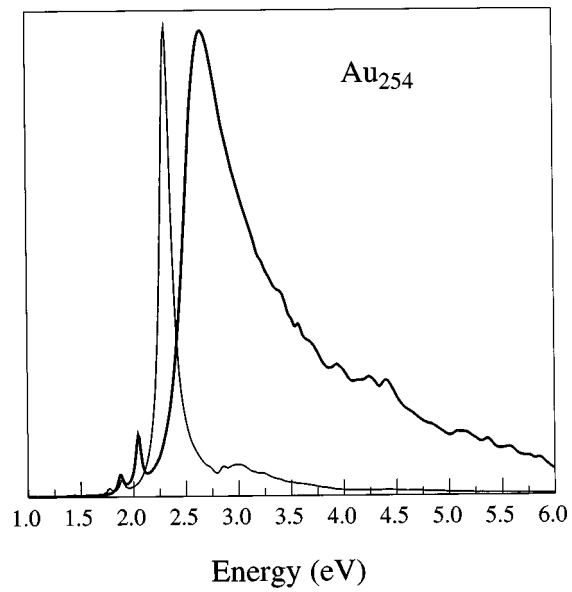

FIG. 5. Theoretical TDLDA absorption spectra of gold clusters in vacuum (thick line curve) and in an alumina matrix (thin line curve). The ''rind'' parameter a, where the screening due to the d electrons is assumed to be ineffective, is equal to 2 a.u. The two curves are independently scaled.

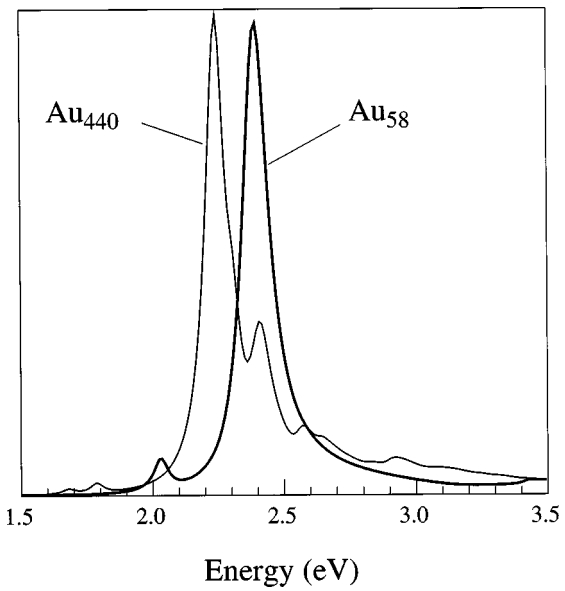

FIG. 6. Theoretical TDLDA absorption spectra of Au_N clusters in an alumina matrix, calculated for two different N values. The ''rind'' parameter a (2 a.u.) is responsible for the blueshift of the plasmon peak with decreasing cluster size. The two curves are independently scaled.

coupling strength with the core-electron absorption [this strength is indeed closely related to $\mathrm{Im}\tilde{\varepsilon}^d(\omega)$] has to be compared with the independent-electron ground-state level width (60 meV) involved for calculating the free response.[52] Moreover, in the presence of dielectric media, the fragmentation due to the residual interaction with the electron-hole excitations (Landau damping) is much less developed than in simple jellium calculations (where $\varepsilon^d=1$ in the full space).

From comparison between TDLDA calculations (Fig. 6) and experiment (Fig. 2), the same global trends can be observed: a blueshift with decreasing cluster size and a plasmon peak frequency in the range 2.0–2.5 eV. However, the TDLDA results lead to a plasmon location at slightly lower energy value (of about 0.2 eV).

Actually the large porosity of the samples is suspected to be responsible for this slight discrepancy. It is likely that at the cluster/matrix interface the porosity is more important because the different chemical nature of both media implies probable defects around the clusters. Model calculations involving a perfect outer rind with $\varepsilon_m=1$ (thickness b on the order or larger than 2 a.u.) yields a plasmon frequency in better agreement with experiment. In fact for large enough b values the free cluster results are recovered. Moreover, when applying the Mie formula for a two-region cluster in vacuum, the plasmon peak is found considerably damped for small radii (the curves look like the experimental ones, exhibiting only a flat shoulder in the plasmon energy range). By contrast the peak is clearly visible over the whole size range when the screening induced by the alumina matrix acts from the cluster boundary, as in the case of the simple Mie formula for a single-region cluster model. In this last case no size-dependent feature occurs, except for the constant R^3 scaling of the absorption spectrum. This last argument is again in favor of the porosity hypothesis.

Details concerning the TDLDA calculations and complete account of the theoretical results will be given in another paper.

VII. CONCLUSION

The low-energy cluster-beam deposition has been proved to be a very efficient technique to prepare optical nanostructures, where at low metal concentration (a few percent) the cluster size can be varied and controlled. In the present paper are reported optical absorption and ellipsometric measurements performed on thin alumina films containing gold clusters in the size range 2–4 nm. The characterization of these composite materials by several complementary techniques shows that the matrix is amorphous and porous, while the metallic particles are spherical and randomly distributed.

Size effects in the optical absorption, as well as in the extracted complex refractive index, are clearly observed. The main features are a blueshift and a damping of the plasmon resonance band with decreasing cluster size. TDLDA calculations allow the understanding of this behavior.

Our technique is clearly not limited to gold particles and many other systems such as silver, copper, and other metals, or semiconductor clusters may be produced in a well-controlled size range, typically between one and a few nanometers.

Ultrafast electron dynamics in such small particles is expected to be a very interesting phenomenon. Femtosecond pump-probe analysis is a powerful method to study the size dependence of the electron-electron and the electron-lattice coupling in the clusters, as has been demonstrated recently with copper.[58]

In the near future we plan to study other systems such as Ag_N clusters and to associate the present optical and ellipsometric observations with such electron dynamics experiments.

ACKNOWLEDGMENTS

The authors are indebted to Dr. A. Gagnaire and co-workers (Ecole Centrale de Lyon) for fruitful collaboration and discussions in the ellipsometric studies. We are also grateful to Professor A. Naudon and co-workers (LMP, Poitiers) for GISAXS measurements at the LURE facility (Orsay). Many thanks to G. Guiraud, F. Valadier, and C. Clavier for their essential technical support.

[1] W. A. de Heer, K. Selby, V. Kresin, J. Masui, M. Vollmer, A. Châtelain, and W. D. Knight, Phys. Rev. Lett. **59**, 1805 (1987).
[2] J. Blanc, V. Bonačić-Koutecký, M. Broyer, J. Chevaleyre, P. Dugourd, J. Koutecký, C. Scheuch, J. P. Wolf, and L. Wöste, J. Chem. Phys. **96**, 1793 (1992).
[3] J. Borggreen, P. Chowdhury, N. Kebaïli, L. Lundsberg-Nielsen, K. Lützenkirchen, M. B. Nielsen, J. Pedersen, and H. D. Rasmussen, Phys. Rev. B **48**, 17 507 (1993).
[4] C. Bréchignac and P. Cahuzac, Comments At. Mol. Phys. **31**, 215 (1995).
[5] T. Reiners, C. Ellert, M. Schmidt, and H. Haberland, Phys. Rev. Lett. **74**, 1558 (1995).
[6] T. Götz, W. Hoheisel, M. Vollmer, and F. Träger, Z. Phys. D **33**, 133 (1995).
[7] U. Kreibig and M. Vollmer, *Optical Properties of Metal Clusters* (Springer, Berlin, 1995).
[8] J. C. Valmalette, L. Lemaire, G. L. Hornyak, J. Dutta, and H. Hofmann, Anal. Mag. **24**, M23 (1996).
[9] T. W. Roberti, B. A. Smith, and J. Z. Zhang, J. Chem. Phys. **102**, 3860 (1995).
[10] P. Mulvaney, Langmuir **12**, 788 (1996).
[11] K. Puech, F. Henari, W. Blau, D. Duff, and G. Schmid, Europhys. Lett. **32**, 119 (1995).
[12] Y. Kobayashi and A. Tomita, J. Colloid Interface Sci. **185**, 285 (1997).
[13] M. Lee, T. S. Kim, and Y. S. Choi, J. Non-Cryst. Solids **211**, 143 (1997).
[14] A. Martino, S. A. Yamanaka, J. S. Kawola, and D. A. Loy, Chem. Mater. **9**, 423 (1997).
[15] Y. Hosoya, T. Suga, T. Yanagawa, and Y. Kurokawa, J. Appl. Phys. **81**, 1475 (1997).
[16] R. L. Whetten, J. T. Khoury, M. M. Alvarez, S. Murthy, I. Vezmar, Z. L. Wang, P. W. Stephens, C. L. Cleveland, W. D. Luedtke, and U. Landman, Adv. Mater. **8**, 428 (1996).
[17] M. M. Alvarez, J. T. Khoury, T. G. Schaaff, M. N. Shafigullin, I. Vezmar, and R. L. Whetten, J. Phys. Chem. B **101**, 3706 (1997).
[18] S. Fedrigo, W. Harbich, and J. Buttet, Phys. Rev. B **47**, 10 706 (1993).
[19] J. Zhao, H. Zhang, and G. Wang, J. Phys. Chem. Solids **57**, 225 (1996).
[20] A. Heilmann, J. Werner, D. Schwarzenberg, S. Henkel, P. Grosse, and W. Theiß, Thin Solid Films **270**, 103 (1995).
[21] H. Ishikawa, T. Ida, and K. Kimura, Surf. Rev. Lett. **3**, 1153 (1996).
[22] C. A. Foss, Jr., G. L. Hornyak, J. A. Stockert, and C. R. Martin, J. Phys. Chem. **98**, 2963 (1994).
[23] G. L. Hornyak, C. J. Patrissi, and C. R. Martin, J. Phys. Chem. B **101**, 1548 (1997).
[24] J. A. Sawicki, G. Abouchacra, J. A. Serughetti, and A. Perez, Nucl. Instrum. Methods Phys. Res. B **16**, 355 (1986).
[25] R. H. Magruder III, L. Yang, R. F. Haglund, Jr., C. W. White, L. Yang, R. Dorsinville, and R. R. Alfano, Appl. Phys. Lett. **62**, 1730 (1993).
[26] R. F. Haglund, Jr., L. Yang, R. H. Magruder III, J. E. Witting, K. Becker, and R. A. Zuhr, Opt. Lett. **18**, 373 (1993).
[27] L. Yang, K. Becker, F. M. Smith, R. H. Magruder III, R. F. Haglund, Jr., L. Yang, R. Dorsinville, R. R. Alfano, and R. A. Zuhr, J. Opt. Soc. Am. B **11**, 457 (1994).
[28] G. A. Niklasson and H. G. Craighead, Thin Solid Films **125**, 165 (1985).
[29] H. Hövel, S. Fritz, A. Hilger, U. Kreibig, and M. Vollmer, Phys. Rev. B **48**, 18 178 (1993).
[30] P. Mélinon, V. Paillard, V. Dupuis, A. Perez, P. Jensen, A. Hoareau, J. P. Perez, J. Tuaillon, M. Broyer, J. L. Vialle, M. Pellarin, B. Baguenard, and J. Lermé, Int. J. Mod. Phys. B **9**, 339 (1995).
[31] A. Perez, P. Mélinon, V. Dupuis, P. Jensen, B. Prével, J. Tuaillon, L. Bardotti, C. Martet, M. Treilleux, M. Broyer, M. Pellarin, J. L. Vialle, B. Palpant, and J. Lermé, J. Phys. D **30**, 709 (1997).
[32] J. C. Maxwell-Garnett, Philos. Trans. R. Soc. London, **203**, 385 (1904); **205**, 237 (1906).
[33] W. D. Knight, K. Clemenger, W. A. de Heer, W. A. Saunders, M. Y. Chou, and M. L. Cohen, Phys. Rev. Lett. **52**, 2141 (1984).
[34] W. Ekardt, Phys. Rev. B **29**, 1558 (1984).
[35] A. Naudon and D. Thiaudière, Surf. Coat. Technol. **79**, 103 (1996).
[36] C. Kittel, *Introduction to Solid State Physics* (John Wiley & Sons, New York, 1983).
[37] G. Mie, Ann. Phys. (Leipzig) **25**, 377 (1908).
[38] D. A. G. Bruggemann, Ann. Phys. (Leipzig) **5**, 636 (1935).
[39] D. J. Bergman, Phys. Rep. **43**, 377 (1978).
[40] P. Chýlek and V. Srivastava, Phys. Rev. B **27**, 5098 (1983).
[41] R. J. Gehr and R. W. Boyd, Chem. Mater. **8**, 1807 (1996).
[42] E. D. Palik, *Handbook of Optical Constants of Solids*, Vols. I and II (Academic Press, New York, 1985/1991).
[43] U. Kreibig, A. Hilger, H. Hövel, and M. Quinten, in *Large Clusters of Atoms and Molecules*, *NATO Advanced Studies Institute Series E: Applied Sciences*, edited by T. P. Martin (Kluwer Academic Publishers, Dordrecht, 1996), p. 475.
[44] Y. Borensztein, P. De Andrès, R. Monreal, T. Lopez-Rios, and F. Flores, Phys. Rev. B **33**, 2828 (1986).
[45] M. Eto and K. Kawamura, Phys. Rev. B **51**, 10 119 (1995).
[46] M. Quinten, Z. Phys. B **101**, 211 (1996).
[47] O. Stenzel and R. Petrich, J. Phys. D **28**, 978 (1995).
[48] R. M. A. Azzam and N. M. Bashara, *Ellipsometry and Polarized Light* (North-Holland, Amsterdam, 1977).
[49] D. E. Aspnes, in *Application of Surface Science* (North-Holland, Amsterdam, 1985), Vols. 22–23, p. 792.
[50] E. Elizalde, J. M. Frigerio, and J. Rivory, Appl. Opt. **25**, 4557 (1986).
[51] W. H. Press, S. A. Teukolsky, W. T. Vetterling, and B. P. Flannery, *Numerical Recipes* (Cambridge University Press, New York, 1992), Chap. 10.

[52] W. Ekardt, Phys. Rev. B **31**, 6360 (1985).
[53] H. Ehrenreich and H. R. Philipp, Phys. Rev. **128**, 1622 (1962).
[54] V. V. Kresin, Phys. Rev. B **51**, 1844 (1995).
[55] A. Liebsch, Phys. Rev. Lett. **71**, 145 (1993); Phys. Rev. B **48**, 11 317 (1993).
[56] Ll. Serra and A. Rubio, Z. Phys. D **40**, 262 (1997).
[57] G. B. Bachelet, D. R. Hamann, and M. Schlüter, Phys. Rev. B **26**, 4199 (1982).
[58] J. Y. Bigot, J. C. Merle, O. Cregut, and A. Daunois, Phys. Rev. Lett. **75**, 4702 (1995).